Sequential Decision Making for Intelligent Agents
Papers from the AAAI 2015 Fall Symposium

Deep Recurrent Q-Learning for Partially Observable MDPs

Matthew Hausknecht and Peter Stone
Department of Computer Science
The University of Texas at Austin
{mhauskn, pstone}@cs.utexas.edu

Abstract

Deep Reinforcement Learning has yielded proficient controllers for complex tasks. However, these controllers have limited memory and rely on being able to perceive the complete game screen at each decision point. To address these shortcomings, this article investigates the effects of adding recurrency to a Deep Q-Network (DQN) by replacing the first post-convolutional fully-connected layer with a recurrent LSTM. The resulting *Deep Recurrent Q-Network* (DRQN), although capable of seeing only a single frame at each timestep, successfully integrates information through time and replicates DQN's performance on standard Atari games and partially observed equivalents featuring flickering game screens. Additionally, when trained with partial observations and evaluated with incrementally more complete observations, DRQN's performance scales as a function of observability. Conversely, when trained with full observations and evaluated with partial observations, DRQN's performance degrades less than DQN's. Thus, given the same length of history, recurrency is a viable alternative to stacking a history of frames in the DQN's input layer and while recurrency confers no systematic advantage when learning to play the game, the recurrent net can better adapt at evaluation time if the quality of observations changes.

Introduction

Deep Q-Networks (DQNs) have been shown to be capable of learning human-level control policies on a variety of different Atari 2600 games (Mnih et al. 2015). True to their name, DQNs learn to estimate the Q-Values (or long-term discounted returns) of selecting each possible action from the current game state. Given that the network's Q-Value estimate is sufficiently accurate, a game may be played by selecting the action with the maximal Q-Value at each timestep. Learning policies mapping from raw screen pixels to actions, these networks have been shown to achieve state-of-the-art performance on many Atari 2600 games.

However, Deep Q-Networks are limited in the sense that they learn a mapping from a limited number of past states, or game screens in the case of Atari 2600. In practice, DQN is trained using an input consisting of the last four states the agent has encountered. Thus DQN will be unable to master games that require the player to remember events more distant than four screens in the past. Put differently, any game that requires a memory of more than four frames will appear non-Markovian to DQN because the future game states (and rewards) depend on more than just DQN's current input. Instead of a Markov Decision Process (MDP), the game becomes a Partially-Observable Markov Decision Process (POMDP).

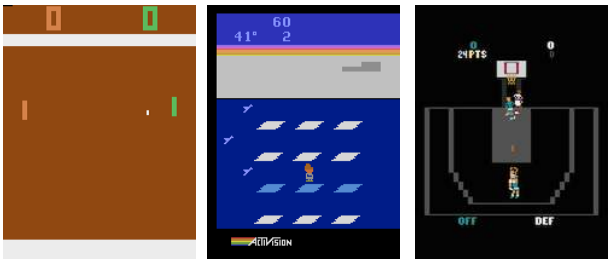

(a) Pong (b) Frostbite (c) Double Dunk

Figure 1: Nearly all Atari 2600 games feature moving objects. Given only one frame of input, Pong, Frostbite, and Double Dunk are all POMDPs because a single observation does not reveal the velocity of the ball (Pong, Double Dunk) or the velocity of the icebergs (Frostbite).

Real-world tasks often feature incomplete and noisy state information resulting from partial observability like that found in POMDPs. As Figure 1 shows, given only a single game screen, many Atari 2600 games are POMDPs. One example is the game of Pong in which the current screen only reveals the location of the paddles and the ball, but not the velocity of the ball. Knowing the direction of travel of the ball is a crucial component for determining the best paddle location.

We observe that DQN's performance declines when given incomplete state observations and hypothesize that DQN may be modified to better deal with POMDPs by leveraging advances in Recurrent Neural Networks. Therefore we introduce the *Deep Recurrent Q-Network* (DRQN), a combination of a Long Short Term Memory (LSTM)(Hochreiter and Schmidhuber 1997) and a Deep Q-Network. Crucially, we demonstrate that DRQN is capable of handling partial

observability, and that recurrency confers benefits when the quality of observations change during evaluation time.

Deep Q-Learning

Reinforcement Learning (Sutton and Barto 1998) is concerned with learning control policies for agents interacting with unknown environments. Such an environment is often formalized as a Markov Decision Process (MDP) which is completely described by a 4-tuple $(\mathcal{S}, \mathcal{A}, \mathcal{P}, \mathcal{R})$. At each timestep t an agent interacting with the MDP observes a state $s_t \in \mathcal{S}$, and chooses an action $a_t \in \mathcal{A}$ which determines the reward $r_t \sim \mathcal{R}(s_t, a_t)$ and next state $s_{t+1} \sim \mathcal{P}(s_t, a_t)$.

Q-Learning (Watkins and Dayan 1992) estimates the value of executing an action from a given state. Such value estimates are referred to as state action values, or sometimes simply Q-values. Q-values are learned iteratively by updating the current Q-value estimate towards the observed reward and estimated utility of the resulting state s':

$$Q(s,a) = Q(s,a) + \alpha\big(r + \gamma \max_{a'} Q(s',a') - Q(s,a)\big) \quad (1)$$

Many challenging domains such as Atari games feature far too many unique states to maintain a separate estimate for each $\mathcal{S} \times \mathcal{A}$. Instead a model is used to approximate the Q-values (Mnih et al. 2015). In the case of Deep Q-Learning, the model is a neural network parameterized by weights and biases collectively denoted as θ. Q-values are estimated online by querying the output nodes of the network after performing a forward pass given a state input. Such Q-values are denoted $Q(s, a|\theta)$. Instead of updating individual Q-values, updates are now made to the parameters of the network to minimize a differentiable loss function:

$$\mathcal{L}(s, a|\theta_i) \approx \big(r + \gamma \max_{a} Q(s', a|\theta_i) - Q(s, a|\theta_i)\big)^2 \quad (2)$$

$$\theta_{i+1} = \theta_i + \alpha \nabla_\theta \mathcal{L}(\theta_i) \quad (3)$$

Since $|\theta| \ll |\mathcal{S} \times \mathcal{A}|$, the neural network model naturally generalizes beyond the states and actions it has been trained on. However, because the same network is both generating the next state target Q-values and updating the current Q-values, updates can adversely affect other Q-value estimates, leading to oscillatory performance or even divergence (Tsitsiklis and Roy 1997). Deep Q-Learning uses three techniques to restore learning stability: First, experiences $e_t = (s_t, a_t, r_t, s_{t+1})$ are recorded in a replay memory $\mathcal{D}$ and then sampled uniformly at training time. Second, a separate, target network $\hat{Q}$ provides stale update targets to the main network. The target network serves to partially decouple the feedback resulting from the network generating its own targets. $\hat{Q}$ is identical to the main network except its parameters θ^- are updated to match θ every 10,000 iterations. Finally, an adaptive learning rate method such as RMSProp (Tieleman and Hinton 2012) or ADADELTA (Zeiler 2012) maintains a per-parameter learning rate α, and adjusts α according to the history of gradient updates to that parameter. This step serves to compensate for the lack of a fixed training dataset; the ever-changing nature of $\mathcal{D}$ may require certain parameters start changing again after having reached a seeming fixed point.

Specifically, at each training iteration i, an experience $e_t = (s_t, a_t, r_t, s_{t+1})$ is sampled uniformly from the replay memory $\mathcal{D}$. The loss of the network is determined as follows:

$$\mathcal{L}_i(\theta_i) = \mathbb{E}_{(s,a,r,s')\sim\mathcal{D}}\left[\Big(y_i - Q(s,a;\theta_i)\Big)^2\right] \quad (4)$$

where $y_i = r + \gamma \max_{a'} \hat{Q}(s', a'; \theta^-)$ is the stale update target given by the target network $\hat{Q}$. Updates performed in this manner have been empirically shown to be tractable and stable (Mnih et al. 2015).

Partial Observability

In real world environments it's rare that the full state of the system can be provided to the agent or even determined. In other words, the Markov property rarely holds in real world environments. A Partially Observable Markov Decision Process (POMDP) better captures the dynamics of many real-world environments by explicitly acknowledging that the sensations received by the agent are only partial glimpses of the underlying system state. Formally a POMDP can be described as a 6-tuple $(\mathcal{S}, \mathcal{A}, \mathcal{P}, \mathcal{R}, \Omega, \mathcal{O})$. $\mathcal{S}, \mathcal{A}, \mathcal{P}, \mathcal{R}$ are the states, actions, transitions, and rewards as before, except now the agent is no longer privy to the true system state and instead receives an observation $o \in \Omega$. This observation is generated from the underlying system state according to the probability distribution $o \sim \mathcal{O}(s)$. Vanilla Deep Q-Learning has no explicit mechanisms for deciphering the underlying state of the POMDP and is only effective if the observations are reflective of underlying system states. In the general case, estimating a Q-value from an observation can be arbitrarily bad since $Q(o, a|\theta) \neq Q(s, a|\theta)$.

Our experiments show that adding recurrency to Deep Q-Learning allows the Q-network network to better estimate the underlying system state, narrowing the gap between $Q(o, a|\theta)$ and $Q(s, a|\theta)$. Stated differently, recurrent deep Q-networks can better approximate actual Q-values from sequences of observations, leading to better policies in partially observed environments.

DRQN Architecture

Depicted in Figure 2, the architecture of DRQN replaces DQN's first fully connected layer with a Long Short Term Memory (Hochreiter and Schmidhuber 1997). For input, the recurrent network takes a single 84×84 preprocessed image, instead of the last four images required by DQN. The first hidden layer convolves 32 8×8 filters with stride 4 across the input image and applies a rectifier nonlinearity. The second hidden layer convolves 64 4×4 filters with stride 2, again followed by a rectifier nonlinearity. The third hidden layer convolves 64 3×3 filters with stride 1, followed by a rectifier. Convolutional outputs are fed to the fully connected LSTM layer. Finally, a fully connected linear layer outputs a Q-Value for each possible action. We settled on

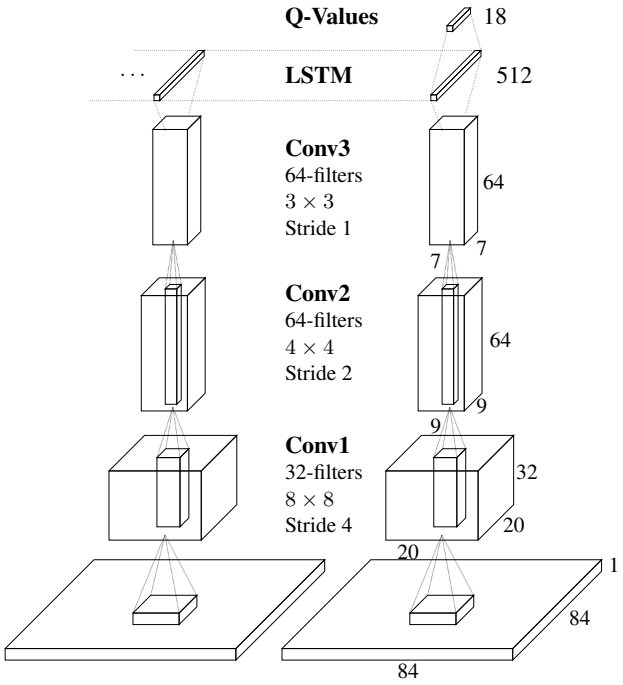

Figure 2: DRQN convolves three times over a single-channel image of the game screen. The resulting activations are processed through time by an LSTM layer. The last two timesteps are shown here. LSTM outputs become Q-Values after passing through a fully-connected layer. Convolutional filters are depicted by rectangular sub-boxes with pointed tops.

this architecture after experimenting with several variations; see Appendix A for details.

Stable Recurrent Updates

Updating a recurrent, convolutional network requires each backward pass to contain many time-steps of game screens and target values. Additionally, the LSTM's initial hidden state may either be zeroed or carried forward from its previous values. We consider two types of updates:

Bootstrapped Sequential Updates: Episodes are selected randomly from the replay memory and updates begin at the beginning of the episode and proceed forward through time to the conclusion of the episode. The targets at each timestep are generated from the target Q-network, $\hat{Q}$. The RNN's hidden state is carried forward throughout the episode.

Bootstrapped Random Updates: Episodes are selected randomly from the replay memory and updates begin at random points in the episode and proceed for only *unroll iterations* timesteps (e.g. one backward call). The targets at each timestep are generated from the target Q-network, $\hat{Q}$. The RNN's initial state is zeroed at the start of the update.

Sequential updates have the advantage of carrying the LSTM's hidden state forward from the beginning of the episode. However, by sampling experiences sequentially for a full episode, they violate DQN's random sampling policy.

Random updates better adhere to the policy of randomly sampling experience, but, as a consequence, the LSTM's hidden state must be zeroed at the start of each update. Zeroing the hidden state makes it harder for the LSTM to learn functions that span longer time scales than the number of timesteps reached by back propagation through time.

Experiments indicate that both types of updates are viable and yield convergent policies with similar performance across a set of games. Therefore, to limit complexity, all results herein use the randomized update strategy. We expect that all presented results would generalize to the case of sequential updates.

Having addressed the architecture and updating of a Deep Recurrent Q-Network, we now show how it performs on domains featuring partial observability.

Atari Games: MDP or POMDP?

The state of an Atari 2600 game is fully described by the 128 bytes of console RAM. Humans and agents, however, observe only the console-generated game screens. For many games, a single game screen is insufficient to determine the state of the system. DQN infers the full state of an Atari game by expanding the state representation to encompass the last four game screens. Many games that were previously POMDPs now become MDPs. Of the 49 games investigated by (Mnih et al. 2015), the authors were unable to identify any that were partially observable given the last four frames of input.[1] In order to introduce partial observability to Atari games without reducing the number of input frames given to DQN, we explore a particular modification to the popular game of Pong.

Flickering Pong POMDP

We introduce the *Flickering Pong* POMDP - a modification to the classic game of Pong such that at each timestep, the screen is either fully revealed or fully obscured with probability $p = 0.5$. Obscuring frames in this manner probabilistically induces an incomplete memory of observations needed for Pong to become a POMDP.

In order to succeed at the game of Flickering Pong, it is necessary to integrate information across frames to estimate relevant variables such as the location and velocity of the ball and the location of the paddle. Since half of the frames are obscured in expectation, a successful player must be robust to the possibility of several potentially contiguous obscured inputs.

We train 3 types of networks to play Flickering Pong: the recurrent 1-frame DRQN, a standard 4-frame DQN, and an augmented 10-frame DQN. As Figure 4a indicates, providing more frames to DQN improves performance. Nevertheless, even with 10 frames of history, DQN still struggles to achieve positive scores.

Perhaps the most important opportunity presented by a history of game screens is the ability to convolutionally detect object velocity. Figure 3 visualizes the game screens

[1] Some Atari games are undoubtedly POMDPs such as Blackjack in which the dealer's cards are hidden from view. Unfortunately, Blackjack is not supported by the ALE emulator.

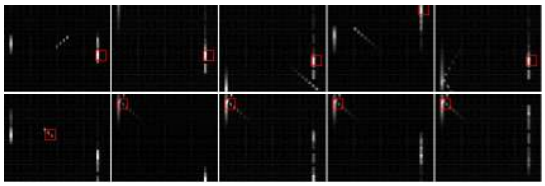

(a) Conv1 Filters

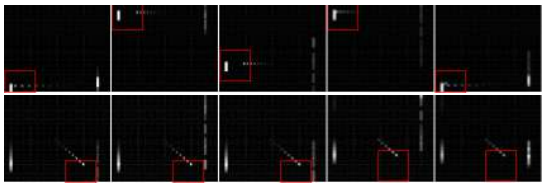

(b) Conv2 Filters

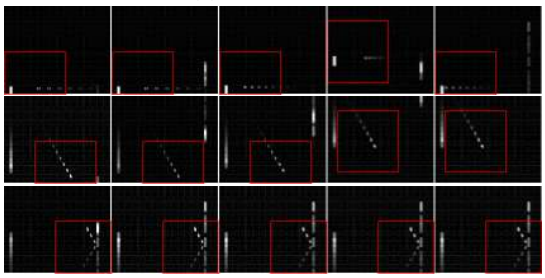

(c) Conv3 Filters

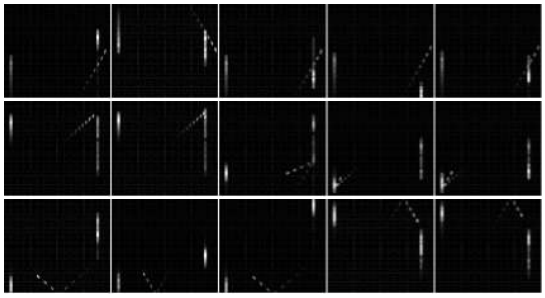

(d) Image sequences maximizing three sample LSTM units

Figure 3: Sample convolution filters learned by 10-frame DQN on the game of Pong. Each row plots the input frames that trigger maximal activation of a particular convolutional filter in the specified layer. The red bounding box illustrates the portion of the input image that caused the maximal activation. Most filters in the first convolutional layer detect only the paddle. Conv2 filters begin to detect ball movement in particular directions and some jointly track the ball and the paddle. Nearly all Conv3 filters track ball and paddle interactions including deflections, ball velocity, and direction of travel. Despite seeing a single frame at a time, individual LSTM units also detect high level events, respectively: the agent missing the ball, ball reflections off of paddles, and ball reflections off the walls. Each image superimposes the last 10-frames seen by the agent, giving more luminance to the more recent frames.

maximizing the activations of different convolutional filters and confirms that 10-frame DQN's filters do detect object velocity, though perhaps less reliably than normal unobscured Pong.[2]

Remarkably, DRQN performs well at this task even when given only one input frame per timestep. With a single frame it is impossible for DRQN's convolutional layers to detect any type of velocity. Instead, the higher-level recurrent layer must compensate for both the flickering game screen and the lack of convolutional velocity detection. Even so, DRQN regularly achieves scores exceeding 10 points out of a maximum of 21. Figure 3d confirms that individual units in the LSTM layer are capable of integrating noisy single-frame information through time to detect high-level Pong events such as the player missing the ball, the ball reflecting on a paddle, or the ball reflecting off the wall.

DRQN is trained using backpropagation through time for the last ten timesteps. Thus both the non-recurrent 10-frame DQN and the recurrent 1-frame DRQN have access to the same history of game screens.[3] DRQN makes better use of the limited history to achieve higher scores.

Thus, when dealing with partial observability, a choice exists between using a non-recurrent deep network with a long history of observations or using a recurrent network trained with a single observation at each timestep. Flickering Pong provides an example in which a recurrent deep network performs better even when given access to the same number of past observations as the non-recurrent network. The performance of DRQN and DQN is further compared across as set of ten games (Table 2), where no systematic advantage is observed for either algorithm.

Generalization Performance

To analyze the generalization performance of the Flickering Pong players, we evaluate the best policies for DRQN, 10-frame DQN, and 4-frame DQN while varying the probability of obscuring the screen. Note that these policies were all trained on Flickering Pong with $p = 0.5$ and are now evaluated against different p values. Figure 4b shows that DRQN performance continues improving as the probability of observing a frame increases. In contrast, 10-frame DQN's performance peaks near the observation probability for which it has been trained and declines even as more frames are observed. Thus DRQN learns a policy which allows performance to scale as a function of observation quality. Such a property is valuable for domains in which the quality of observations varies through time.

Can DRQN Mimic an Unobscured Pong player?

In order to better understand the mechanisms that allow DRQN to function well in the Flickering Pong environment, we analyze the differences between a flicker-trained DRQN player when playing the same trajectory of Pong at $p = 0.5$ and $p = 1.0$, with the hypothesis that if the flickering-Pong agent can infer the underlying game state in obscured screens, its activations should mirror those of the unobscured

[2](Guo et al. 2014) also confirms that convolutional filters learn to respond to patterns of movement seen in game objects.

[3]However, (Karpathy, Johnson, and Li 2015) show that LSTMs can learn functions at training time over a limited set of timesteps and then generalize them at test time to longer sequences.

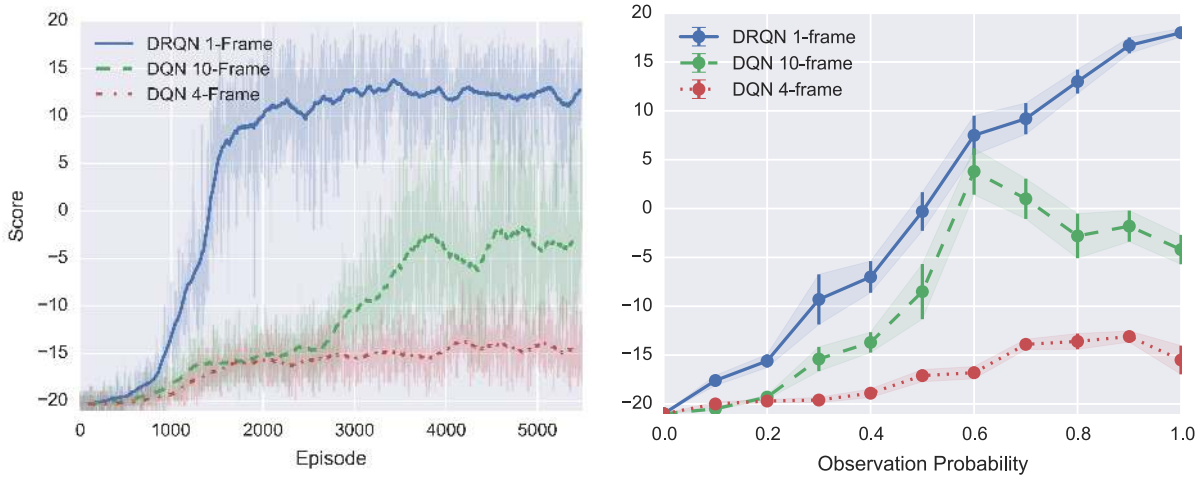

(a) Flickering Pong

(b) Policy Generalization

Figure 4: **Left:** In the partially-observable *Flickering Pong* environment, DRQN proves far more capable at handling the noisy sensations than DQN despite having only a single frame of input. Lacking recurrency, 4-frame DQN struggles to overcome the partial observability induced by the flickering game screen. This struggle is partially remedied by providing DQN with 10-frames of history. **Right:** After being trained with observation probability of 0.5, the learned policies are then tested for generalization. The policies learned by DRQN generalize gracefully to different observation probabilities. DQN's performance peaks slightly above the probability on which it was trained. Errorbars denote standard error.

$p = 1.0$ agent. We use normalized Euclidean distance as a metric to quantify the difference between two vectors of activations $\mathbf{u}, \mathbf{v}$:

$$E(\mathbf{u}, \mathbf{v}) = \frac{1}{2\,|\mathbf{u}|}\|\mathbf{u} - \mathbf{v}\|_2^2 \tag{5}$$

Let us denote the vector of activations of DRQN's LSTM-layer at timestep t when playing a game of Flickering Pong as $\mathbf{h}_t^{\mathcal{O}}$. When flicker is disabled and the full state is revealed, we denote the activations as $\mathbf{h}_t^{\mathcal{S}}$. We allow the Flickering Pong player to play ten games and record the values of the LSTM layer $[\mathbf{h}_1^{\mathcal{O}} \ldots \mathbf{h}_T^{\mathcal{O}}]$. Next, we evaluate the same network over the same 10-game trajectory but with all frames revealed to get $[\mathbf{h}_1^{\mathcal{S}} \ldots \mathbf{h}_T^{\mathcal{S}}]$. If the LSTM is capable of inferring the game state even when the screen is unobserved, one would expect the average Euclidean distance between $E(\mathbf{h}_t^{\mathcal{O}}, \mathbf{h}_t^{\mathcal{S}})$ to be low for all t in which the screen is obscured. Figures 5a-5b plot this quantity as a function of the number of consecutive obscured frames for both DRQN and 10-frame DQN.[4] Compared to DQN, DRQN has a much smaller average distance between its activations when playing a game of Flickering Pong and a game of unobscured Pong. Additionally, DRQNs activations change smoothly even in the presence of noise.

However, simply comparing the Euclidean distance does not tell the full story since 10-frame DQN could just have a larger expected frame-to-frame change in activations than DRQN. To control for this, Figures 5a-5b additionally plot the overall change in activations since the last observed frame, $E(\mathbf{h}_t^{\mathcal{O}}, \mathbf{h}_{t-i}^{\mathcal{O}})$. This measure gives a sense of the overall timestep-to-timestep volatility of activations.

Finally, when the screen is obscured, it is expected that the network's activations will change. What is of interest is whether they change in the same direction as the activations of the unobscured network. Let $\mathcal{A}_i$ denotes the set of all timesteps in the trajectory in which the last i screens have been obscured. We then examine the average ratio of distance between the obscured and unobscured activations divided by the distance between the obscured activation in the current timestep and the last timestep that the game screen was observed:

$$\text{Loss Ratio}_i = \frac{1}{|\mathcal{A}_i|}\sum_{t \in \mathcal{A}_i} \frac{E(\mathbf{h}_t^{\mathcal{S}}, \mathbf{h}_t^{\mathcal{O}})}{E(\mathbf{h}_t^{\mathcal{O}}, \mathbf{h}_{t-i}^{\mathcal{O}})} \tag{6}$$

Lower values of Loss Ratio indicate the degree to which the obscured network's activations are not only changing, but changing in the same direction as the unobscured network (e.g. the extent to which the obscured player can infer the game state despite not seeing the screen). As Figure 5c shows, DRQN has a lower loss ratio than DQN over all values of consecutive obscured frames, indicating that it better mimics the unobscured network's activations. Since Flickering Pong genuinely discards information each time a screen is obscured, it is reasonable to expect some distance between the activations of obscured and unobscured player. Indeed, DRQN's obscured-screen activations are roughly equidistant from both the unobscured activations and the activations

[4] Since 10-frame DQN has no LSTM layer, Euclidean distance is computed over the activations of the first post-convolutional fully-connected layer. This layer has 512 units as does DRQN's LSTM layer.

	DRQN $\pm std$	DQN $\pm std$	
Game		Ours	Mnih et al.
Asteroids	1020 ($\pm$312)	1070 ($\pm$345)	1629 ($\pm$542)
Beam Rider	3269 ($\pm$1167)	**6923** ($\pm$1027)	6846 ($\pm$1619)
Bowling	62 ($\pm$5.9)	72 ($\pm$11)	42 ($\pm$88)
Centipede	3534 ($\pm$1601)	3653 ($\pm$1903)	8309 ($\pm$5237)
Chopper Cmd	2070 ($\pm$875)	1460 ($\pm$976)	6687 ($\pm$2916)
Double Dunk	**-2** ($\pm$7.8)	-10 ($\pm$3.5)	-18.1 ($\pm$2.6)
Frostbite	**2875** ($\pm$535)	519 ($\pm$363)	328.3 ($\pm$250.5)
Ice Hockey	-4.4 ($\pm$1.6)	-3.5 ($\pm$3.5)	-1.6 ($\pm$2.5)
Ms. Pacman	2048 ($\pm$653)	2363 ($\pm$735)	2311 ($\pm$525)

Table 1: On standard Atari games, DRQN performance parallels DQN, excelling in the games of Frostbite and Double Dunk, but struggling on Beam Rider. Bolded font indicates statistical significance between DRQN and our DQN.[5]

of the last observed screen, meaning that upon encountering an obscured screen, DRQN cannot fully infer the hidden game state. However, nor does it fully preserve its past activations.

Evaluation on Standard Atari Games

We selected the following nine Atari games for evaluation: *Asteroids* and *Double Dunk* feature naturally-flickering sprites making them good potential candidates for recurrent learning. *Beam Rider*, *Centipede*, and *Chopper Command* are shooters. *Frostbite* is a platformer similar to Frogger. *Ice Hockey* and *Double Dunk* are sports games that require positioning players, passing and shooting the puck/ball, and require the player to be capable of both offense and defense. *Bowling* requires actions to be taken at a specific time in order to guide the ball. *Ms Pacman* features flickering ghosts and power pills.

Given the last four frames of input, all of these games are MDPs rather than POMDPs. Thus there is no reason to expect DRQN to outperform DQN. Indeed, results in Table 1 indicate that on average, DRQN does roughly as well DQN. Specifically, our re-implementation of DQN performs similarly to the original, outperforming the original on five out of the nine games, but achieving less than half the original score on Centipede and Chopper Command. DRQN performs outperforms our DQN on the games of Frostbite and Double Dunk, but does significantly worse on the game of Beam Rider (Figure 6). The game of Frostbite (Figure 1b) requires the player to jump across all four rows of moving icebergs and return to the top of the screen. After traversing the icebergs several times, enough ice has been collected to build and igloo at the top right of the screen. Subsequently the player can enter the igloo to advance to the next level. As shown in Figure 6, after 12,000 episodes DRQN discovers a policy that allows it to reliably advance past the first level of Frostbite. For experimental details, see Appendix C.

MDP to POMDP Generalization

Figure 4b shows that DRQN performance increases when trained on a POMDP and then evaluated on a MDP. Arguably the more interesting question is the reverse: can a recurrent network be trained on a standard MDP and then generalize to a POMDP at evaluation time? To address this question, we evaluate the highest-scoring policies of DRQN and DQN over the flickering equivalents of all 9 games in Table 1. Figure 7 shows that while both algorithms incur significant performance decreases on account of the missing information, DRQN captures more of its previous performance than DQN across all levels of flickering. We conclude that recurrent controllers have a certain degree of robustness against missing information, even trained with full state information.

[5]Statistical significance of scores determined by independent t-tests using Benjamini-Hochberg procedure and significance level $P = .05$.

Flickering	DRQN $\pm std$	DQN $\pm std$
Asteroids	1032 ($\pm$410)	1010 ($\pm$535)
Beam Rider	618 ($\pm$115)	**1685.6** ($\pm$875)
Bowling	65.5 ($\pm$13)	57.3 ($\pm$8)
Centipede	4319.2 ($\pm$4378)	5268.1 ($\pm$2052)
Chopper Cmd	1330 ($\pm$294)	1450 ($\pm$787.8)
Double Dunk	-14 ($\pm$2.5)	-16.2 ($\pm$2.6)
Frostbite	414 ($\pm$494)	436 ($\pm$462.5)
Ice Hockey	-5.4 ($\pm$2.7)	-4.2 ($\pm$1.5)
Ms. Pacman	1739 ($\pm$942)	1824 ($\pm$490)
Pong	**12.1** ($\pm$2.2)	-9.9 ($\pm$3.3)

Table 2: Each screen is obscured with probability 0.5, resulting in a partially-observable, flickering equivalent of the standard game. Bold font indicates statistical significance.[5]

Related Work

Previously, LSTM networks have been demonstrated to solve POMDPs when trained using policy gradient methods (Wierstra et al. 2007). In contrast to policy gradient, our work uses temporal-difference updates to bootstrap an action-value function. Additionally, by jointly training convolutional and LSTM layers we are able to learn directly from pixels and do not require hand-engineered features.

LSTM has been used as an advantage-function approximator and shown to solve a partially observable corridor and cartpole tasks better better than comparable (non-LSTM) RNNs (Bakker 2001). While similar in principle, the corridor and cartpole tasks feature tiny states spaces with just a few features.

In parallel to our work, (Narasimhan, Kulkarni, and Barzilay 2015) independently combined LSTM with Deep Reinforcement Learning to demonstrate that recurrency helps to better play text-based fantasy games. The approach is similar but the domains differ: despite the apparent complexity of the fantasy-generated text, the underlying MDPs feature relatively low-dimensional manifolds of underlying state space. The more complex of the two games features only 56 underlying states. Atari games, in contrast, feature a much richer state space with typical games having millions of different states. However, the action space of the text games is much larger with a branching factor of 222 versus Atari's 18.

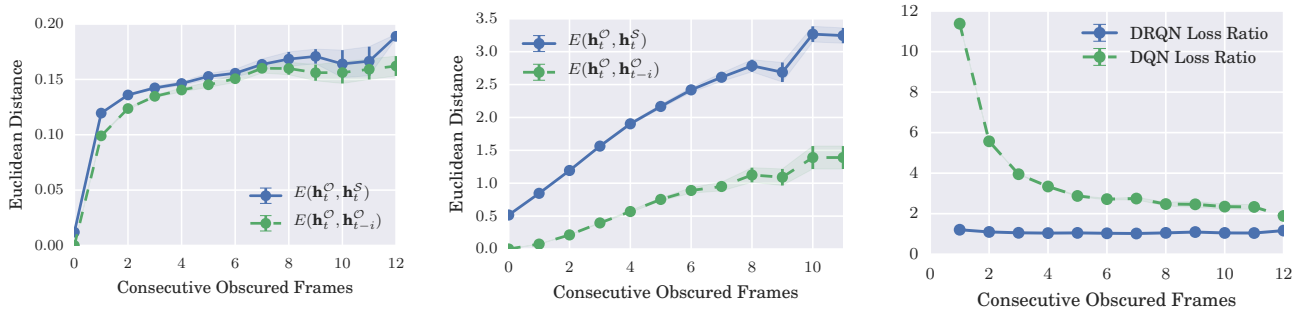

(a) DRQN (b) DQN (c) Loss Ratio

Figure 5: The left two subplots show the average Euclidean distance between the un-obscured and the obscured network's activations $E(\mathbf{h}_t^{\mathcal{O}}, \mathbf{h}_t^{S})$ as a function of the number of consecutive obscured game screens. $E(\mathbf{h}_t^{\mathcal{O}}, \mathbf{h}_{t-i}^{\mathcal{O}})$ shows the Euclidean distance between the networks current activations and those at the last timestep in which the screen was observed. The right subplot shows the ratio of these two quantities, showing that when game screens are obscured, DRQN's activations much more closely follow the activations of the un-obscured player than do DQN's activations.

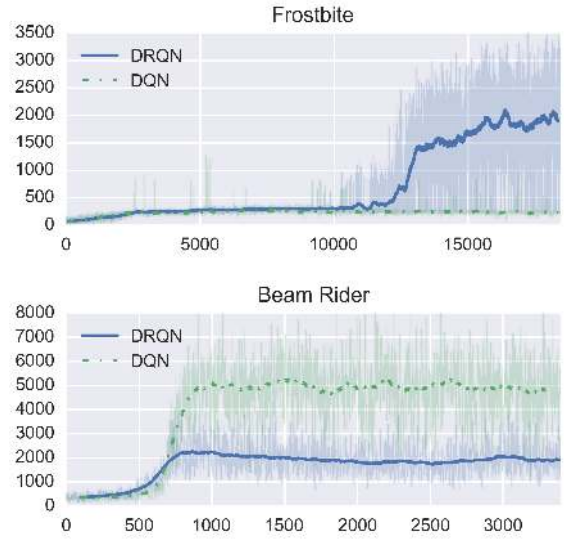

Figure 6: Frostbite and Beam Rider represent the best and worst games for DRQN. Frostbite performance jumps as the agent learns to reliably complete the first level.

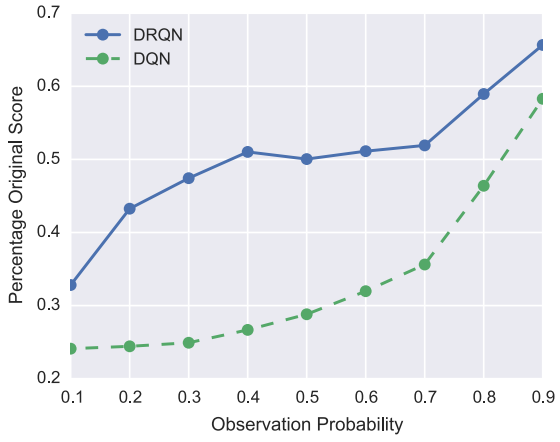

Figure 7: When trained on normal games (MDPs) and then evaluated on flickering games (POMDPs), DRQN's performance degrades more gracefully than DQN's. Each data point shows the average percentage of the original game score over all 9 games in Table 1.

Discussion and Conclusion

Real-world tasks often feature incomplete and noisy state information, resulting from partial observability. We modify DQN to handle the noisy observations characteristic of POMDPs by combining a Long Short Term Memory with a Deep Q-Network. The resulting *Deep Recurrent Q-Network* (DRQN), despite seeing only a single frame at each step, is still capable integrating information across frames to detect relevant information such as velocity of on-screen objects. Additionally, on the game of Pong, DRQN is better equipped than a standard Deep Q-Network to handle the type of partial observability induced by flickering game screens.

Further analysis shows that DRQN, when trained with partial observations, can generalize its policies to the case of complete observations. On the Flickering Pong domain, performance scales with the observability of the domain, reaching near-perfect levels when every game screen is observed. This result indicates that the recurrent network learns policies that are both robust enough to handle to missing game screens, and scalable enough to improve performance as more data becomes available. Generalization also occurs in the opposite direction: when trained on standard Atari games and evaluated against flickering games, DRQN's performance generalizes better than DQN's at all levels of partial information.

Our experiments suggest that Pong represents an outlier among the examined games. Across a set of ten Flicker-

ing MDPs we observe no systematic improvement when employing recurrency. Similarly, across non-flickering Atari games, there are few significant differences between the recurrent and non-recurrent player. This observation leads us to conclude that while recurrency is a viable method for handling multiple state observations, it confers no systematic benefit compared to stacking the observations in the input layer of a convolutional network. An interesting avenue for future is to identify the relevant characteristics of the Pong and Frostbite domains that lead to better performance by recurrent networks.

Acknowledgments

This work has taken place in the Learning Agents Research Group (LARG) at the Artificial Intelligence Laboratory, The University of Texas at Austin. LARG research is supported in part by grants from the National Science Foundation (CNS-1330072, CNS-1305287), ONR (21C184-01), AFRL (FA8750-14-1-0070), AFOSR (FA9550-14-1-0087), and Yujin Robot. Additional support from the Texas Advanced Computing Center, and Nvidia Corporation.

References

Bakker, B. 2001. Reinforcement learning with long short-term memory. In *NIPS*, 1475–1482. MIT Press.

Bellemare, M. G.; Naddaf, Y.; Veness, J.; and Bowling, M. 2013. The arcade learning environment: An evaluation platform for general agents. *Journal of Artificial Intelligence Research* 47:253–279.

Guo, X.; Singh, S.; Lee, H.; Lewis, R. L.; and Wang, X. 2014. Deep learning for real-time atari game play using offline monte-carlo tree search planning. In Ghahramani, Z.; Welling, M.; Cortes, C.; Lawrence, N.; and Weinberger, K., eds., *Advances in Neural Information Processing Systems 27*. Curran Associates, Inc. 3338–3346.

Hochreiter, S., and Schmidhuber, J. 1997. Long short-term memory. *Neural Comput.* 9(8):1735–1780.

Jia, Y.; Shelhamer, E.; Donahue, J.; Karayev, S.; Long, J.; Girshick, R.; Guadarrama, S.; and Darrell, T. 2014. Caffe: Convolutional architecture for fast feature embedding. *arXiv preprint arXiv:1408.5093*.

Karpathy, A.; Johnson, J.; and Li, F.-F. 2015. Visualizing and understanding recurrent networks. *arXiv preprint*.

Mnih, V.; Kavukcuoglu, K.; Silver, D.; Rusu, A. A.; Veness, J.; Bellemare, M. G.; Graves, A.; Riedmiller, M.; Fidjeland, A. K.; Ostrovski, G.; Petersen, S.; Beattie, C.; Sadik, A.; Antonoglou, I.; King, H.; Kumaran, D.; Wierstra, D.; Legg, S.; and Hassabis, D. 2015. Human-level control through deep reinforcement learning. *Nature* 518(7540):529–533.

Narasimhan, K.; Kulkarni, T.; and Barzilay, R. 2015. Language understanding for text-based games using deep reinforcement learning. *CoRR* abs/1506.08941.

Sutton, R. S., and Barto, A. G. 1998. *Reinforcement Learning: An Introduction*. MIT Press.

Tieleman, T., and Hinton, G. 2012. Lecture 6.5—RmsProp: Divide the gradient by a running average of its recent magnitude. COURSERA: Neural Networks for Machine Learning.

Tsitsiklis, J. N., and Roy, B. V. 1997. An analysis of temporal-difference learning with function approximation. *IEEE Transactions on Automatic Control* 42(5):674–690.

Watkins, C. J. C. H., and Dayan, P. 1992. Q-learning. *Machine Learning* 8(3-4):279–292.

Wierstra, D.; Foerster, A.; Peters, J.; and Schmidthuber, J. 2007. Solving deep memory POMDPs with recurrent policy gradients.

Zeiler, M. D. 2012. ADADELTA: An adaptive learning rate method. *CoRR* abs/1212.5701.

Appendix A: Alternative Architectures

Several alternative architectures were evaluated on the game of Beam Rider. We explored the possibility of either replacing the first non-convolutional fully connected layer with an LSTM layer (LSTM replaces IP1) or adding the LSTM layer between the first and second fully connected layers (LSTM over IP1). Results strongly indicated LSTM should replace IP1. We hypothesize this allows LSTM direct access to the convolutional features. Additionally, adding a Rectifier layer after the LSTM layer consistently reduced performance.

Description	Percent Improvement
LSTM replaces IP1	709%
ReLU-LSTM replaces IP1	533%
LSTM over IP1	418%
ReLU-LSTM over IP1	0%

Appendix B: Computational Efficiency

Computational efficiency of RNNs is an important concern. We conducted experiments by performing 1000 backwards and forwards passes and reporting the average time in milliseconds required for each pass. Experiments used a single Nvidia GTX Titan Black using CuDNN and a fully optimized version of Caffe. Results indicate that computation scales sub-linearly in both the number of frames stacked in the input layer and the number of iterations unrolled. Even so, models trained on a large number of stacked frames and unrolled for many iterations are often computationally intractable. For example a model unrolled for 30 iterations with 10 stacked frames would require over 56 days to reach 10 million iterations.

	Backwards (ms)			Forwards (ms)		
Frames	1	4	10	1	4	10
Baseline	8.82	13.6	26.7	2.0	4.0	9.0
Unroll 1	18.2	22.3	33.7	2.4	4.4	9.4
Unroll 10	77.3	111.3	180.5	2.5	4.4	8.3
Unroll 30	204.5	263.4	491.1	2.5	3.8	9.4

Table 3: Average milliseconds per backwards/forwards pass. Frames refers to the number of channels in the input image. Baseline is a non recurrent network (e.g. DQN). Unroll refers to an LSTM network backpropagated through time $1/10/30$ steps.

Appendix C: Experimental Details

Policies were evaluated every 50,000 iterations by playing 10 episodes and averaging the resulting scores. Networks were trained for 10 million iterations and used a replay memory of size 400,000. Additionally, all networks used ADADELTA (Zeiler 2012) optimizer with a learning rate of 0.1 and momentum of 0.95. LSTM's gradients were clipped to a value of ten to ensure learning stability. All other settings were identical to those given in (Mnih et al. 2015).

All networks were trained using the Arcade Learning Environment ALE (Bellemare et al. 2013). The following ALE options were used: color averaging, minimal action set, and death detection.

DRQN is implemented in Caffe (Jia et al. 2014). The source is available at https://github.com/mhauskn/dqn/tree/recurrent.